Journal of Statistical Mechanics: Theory and Experiment
An IOP and SISSA journal

Mixing effectiveness depends on the source–sink structure: simulation results

Takahide Okabe[1], Bruno Eckhardt[2], Jean-Luc Thiffeault[3] and Charles R Doering[4]

[1] Department of Physics and Institute for Fusion Studies, The University of Texas at Austin, Austin, TX 78712-0264, USA
[2] Fachbereich Physik, Philipps-Universtität, D-35032 Marburg, Germany
[3] Department of Mathematics, University of Wisconsin—Madison, Madison, WI 53706-1388, USA
[4] Departments of Mathematics and Physics, University of Michigan, Ann Arbor, MI 48109-1043, USA
E-mail: okabet@mail.utexas.edu, bruno.eckhardt@physik.uni-marburg.de, jeanluc@mailaps.org and doering@umich.edu

Received 18 April 2008
Accepted 1 July 2008
Published 21 July 2008

Online at stacks.iop.org/JSTAT/2008/P07018
doi:10.1088/1742-5468/2008/07/P07018

Abstract. Mixing refers to the homogenization of concentrations of passive scalars in fluids. On small scales it is dominated by diffusion and on large scales it is assisted by stirring. In the presence of scalar sources and sinks the concentration field remains inhomogeneous, but the combined effect of stirring and dissipation may lead to a statistically stationary state. One measure of the quality of mixing is then the standard deviation of the scalar concentration from the mean, and the effectiveness of a stirring velocity field can be gauged by comparing the concentration fluctuations in the presence of stirring to those in its absence. It was recently noted that the maximum possible effectiveness of any stirring depends on the detailed structure of the sources and sinks. We present results from particle-based simulations that confirm this strong source–sink dependence of the mixing enhancement by stirring.

Keywords: stochastic particle dynamics (theory), transport processes/heat transfer (theory), Brownian motion, turbulence

ArXiv ePrint: 0804.2805

1742-5468/08/P07018+13$30.00

Contents

1. Introduction

Mixing by fluid flows is a ubiquitous natural phenomenon that plays a central role in many of the applied sciences and engineering. A geophysical example is the mixing of aerosols (e.g., CO_2 supplied by a volcano, say, or by human activity) in the atmosphere. Aerosols are dispersed by molecular diffusion on the smallest scales but are more effectively spread globally by atmospheric flows. The density—and density fluctuations—of some aerosols influence the albedo of the Earth and thus have a significant environmental impact. Hence it is important to understand fundamental properties of dispersion, mixing, and the reduction of concentration fluctuations produced by stirring flow fields.

Various aspects of mixing have been the focus of many review articles [1]–[8]. At the most basic level, the mixing of a passive scalar can be modeled by an advection–diffusion equation for the scalar concentration field with a specified stirring flow field. In this work we will focus on problems where fluctuations in the scalar field are generated and sustained by temporally steady but spatially inhomogeneous sources. The question of interest here is this: for a given source distribution, how well can a specified stirring flow mix the scalar field?

Mixing effectiveness can be measured by the scalar variance over the domain. A well-mixed scalar field will have a more uniform density with relatively 'small' variance while increased fluctuations in the scalar density will be reflected in a 'large' variance. We put quotes around the quantifiers small and large because the variance is a dimensional quantity that needs an appropriate dimensional point of reference from which it is being measured.

Several years ago Thiffeault *et al* [9] introduced a notion of 'mixing enhancement' for a velocity field stirring a steadily sustained scalar by comparing the bulk (space–time) averaged density variance with and without advecting flow. Mixing is accomplished by molecular diffusion alone in the absence of stirring, which can be quite effective on small scales but is not generally so good at breaking up and dispersing large scale fluctuations quickly. Stirring can greatly enhance the transport of the scalar from regions of excess

J. Stat. Mech. (2008) P07018

density to depleted regions, suppressing the variance far below its diffusion-only value. The magnitude of this variance suppression by the stirring—the ratio of the variance without stirring to the variance in the presence of stirring—is a dimensionless quantity that provides a sensible gauge of the mixing effectiveness of the flow. Different advection fields will have different mixing efficiency stirring scalars supplied by different sources. It is then of obvious interest both to determine theoretical limits on mixing enhancements for various source configurations and to explore whether those limits may be approached—or even perhaps achieved—for particular flows.

There have been many studies of stirring and mixing of a scalar with fluctuations sustained by spatially inhomogeneous sources and sinks. Some of the earliest are by Townsend [10, 11], who was concerned with the effect of turbulence and molecular diffusion on a heated filament. He found that the spatial localization of the source enhanced the role of molecular diffusivity. Durbin [12] and Drummond [13] introduced stochastic particle models to turbulence modeling, and these allowed more detailed studies of the effect of the source on diffusion. Sawford and Hunt [14] pointed out that small sources lead to a dependence of the variance on molecular diffusivity. These models were further refined by [5, 15, 16]. Chertkov *et al* [17]–[21] and Balkovsky and Fouxon [22] addressed the case of a random, statistically steady source.

In this paper we study the enhancement of mixing by an advection field using a particle-based computational scheme that is easy to implement and applicable to a variety of source distributions. The idea is to develop a method that accurately simulates advection and diffusion of large numbers of particles supplied by a steady source, and to measure density fluctuations by 'binning' the particles to produce an approximation of the hydrodynamic concentration field. Unlike a numerical PDE code, a particle code does not favor specific forms of the flow or the source (PDE methods generally work best with very smooth fields). There is, however, no free lunch: the accuracy of the particle code is ultimately limited by the finite number of particles that can be tracked. The limitation to finite numbers of particles inevitably introduces statistical errors due to discrete fluctuations in the local density and systematic errors in the variance measurements due to binning. But these problems are tractable, and as we will show, the method proves to be quantitatively accurate and computationally efficient for some applications.

2. Theoretical background

In this section we review basic facts about the mixing enhancement problem as formulated by Thiffeault, Doering and Gibbon *et al* [9] and developed by Plasting and Young [23], Doering and Thiffeault [24], Shaw *et al* [25], and Thiffeault and Pavliotis [26]. The dynamics is given by the advection–diffusion equation for the concentration of a passive scalar $\rho(t, \boldsymbol{x})$ with time-independent but spatially inhomogeneous source field $S(\boldsymbol{x})$:

$$\frac{\partial \rho}{\partial t} + \boldsymbol{u} \cdot \nabla \rho = \kappa \Delta \rho + S(\boldsymbol{x}), \tag{1}$$

where κ is the molecular diffusivity and $\boldsymbol{u}(t, \boldsymbol{x})$ is a specified advection field that satisfies (at each instant of time) the incompressibility condition

$$\nabla \cdot \boldsymbol{u} = 0. \tag{2}$$

J. Stat. Mech. (2008) P07018

For simplicity, the domain is the d-torus, i.e., $[0, L]^d$ with periodic boundary conditions. We limit attention to stirring fields that satisfy the properties of statistical homogeneity and isotropy in space defined by

$$\overline{u_i(\cdot, \boldsymbol{x})} = 0, \qquad \overline{u_i(\cdot, \boldsymbol{x}) u_j(\cdot, \boldsymbol{x})} = \frac{U^2}{d} \delta_{ij}, \tag{3}$$

where the overbar denotes time averaging and U is the root mean square speed of the velocity field, a natural indicator of the intensity of the stirring. These are statistical properties of homogeneous isotropic turbulence on the torus, but they are also shared by many other kinds of flows.

We are interested in fluctuations in the concentration ρ so the spatially averaged background density is irrelevant. It is easy to see from (1) that the spatial average of ρ grows linearly with time at the rate given by the spatial average of S. Hence we change variables to spatially mean-zero quantities

$$\theta(t, \boldsymbol{x}) = \rho(t, \boldsymbol{x}) - \frac{1}{L^d} \int \mathrm{d}^d x' \, \rho(t, \boldsymbol{x}') \tag{4}$$

and

$$s(\boldsymbol{x}) = S(\boldsymbol{x}) - \frac{1}{L^d} \int \mathrm{d}^d x' \, S(\boldsymbol{x}') \tag{5}$$

that satisfy

$$\frac{\partial \theta}{\partial t} + \boldsymbol{u} \cdot \nabla \theta = \kappa \Delta \theta + s(\boldsymbol{x}). \tag{6}$$

(We must also supply initial conditions for ρ and/or θ but they play no role in the long time steady statistics that we are interested in.)

The 'mixedness' of the scalar may be characterized by, among other quantities, the long time averaged variance of ρ, proportional to the long time averaged L^2 norm of θ,

$$\langle \theta^2 \rangle := \lim_{T \to \infty} \frac{1}{T} \int_0^T \mathrm{d}t \, \frac{1}{L^d} \int \mathrm{d}^d x \, \theta^2(t, \boldsymbol{x}). \tag{7}$$

The smaller $\langle \theta^2 \rangle$ is, the more uniform the distribution. The 'mixing enhancement' of a stirring field is naturally measured by comparing the scalar variance to the variance with the same source but in the absence of stirring. To be precise, we compare $\langle \theta^2 \rangle$ to $\langle \theta_0^2 \rangle$ where θ_0 is the solution to

$$\frac{\partial \theta_0}{\partial t} = \kappa \Delta \theta_0 + s(\boldsymbol{x}) \tag{8}$$

(with, say, the same initial data although these will not affect the long time averaged fluctuations). The dimensionless *mixing enhancement factor* is then defined as

$$\mathcal{E}_0 := \sqrt{\frac{\langle \theta_0^2 \rangle}{\langle \theta^2 \rangle}}. \tag{9}$$

This quantity carries the subscript 0 because we can also define *multiscale mixing enhancements* [24, 25] by weighting large/small wavenumber components of the

J. Stat. Mech. (2008) P07018

scalar fluctuations:

$$\mathcal{E}_p := \sqrt{\frac{\langle|\nabla^p\theta_0|^2\rangle}{\langle|\nabla^p\theta|^2\rangle}}, \qquad p=-1,0,1. \tag{10}$$

As discussed in Doering and Thiffeault [24], Shaw *et al* [25] and Shaw [27], $\mathcal{E}_{\pm1}$ provide a gauge of the mixing enhancement of the flow as measured by scalar fluctuations on relatively small and large length scales, respectively. We refer to them as enhancement factors because if one were to define an effective, eddy, or equivalent diffusivity $\kappa_{\mathrm{e},p}$ as the value of a molecular diffusion coefficient necessary to produce the same value of $\langle|\nabla^p\theta|^2\rangle$ with stirring, then we would have $\kappa_{\mathrm{e},p} = \kappa\mathcal{E}_p$. In this paper, however, we will focus exclusively on $\mathcal{E}_0$, the mixing enhancement at 'moderate' length scales.

There is a theoretical upper bound on $\mathcal{E}_0$ valid for any statistically stationary homogeneous and isotropic stirring field [24, 25, 27]:

$$\mathcal{E}_0 \le \sqrt{\frac{\sum_{\boldsymbol{k}\neq\boldsymbol{0}}|\hat{s}(\boldsymbol{k})|^2/k^4}{\sum_{\boldsymbol{k}\neq\boldsymbol{0}}|\hat{s}(\boldsymbol{k})|^2/(k^4+Pe^2/L^2dk^2)}}, \tag{11}$$

where $\hat{s}(\boldsymbol{k})$ are the Fourier coefficients of the source and the Péclet number,

$$Pe := UL/\kappa, \tag{12}$$

is a dimensionless measure of the intensity of the stirring. Generally, we anticipate that $\mathcal{E}_0$ is an increasing function of Pe and the estimate in (11) guarantees that $\mathcal{E}_0(Pe) \lesssim Pe$ as $Pe\to\infty$, the 'classical' scaling necessary if there is to be any residual variance suppression in the singular vanishing diffusion limit. That is, if $\mathcal{E}_0(Pe)\sim Pe$ then $\kappa_{\mathrm{e},0}$ has a non-zero limit as $\kappa\to 0$ with all other parameters held fixed. It is natural to refer to any of the possible subclassical scalings as 'anomalous'.

The upper limit to the mixing enhancement in (11) depends on the stirring field only through U via Pe, but it depends on all the details of the source distribution. As studied in depth in [24, 25, 27], the structure of the scalar source can have a profound effect on the high Pe scaling of $\mathcal{E}_0$, notably for sources with small scales. It is physically meaningful to consider measure-valued source–sink distributions, like delta functions, with arbitrarily small scales. It is precisely this source size dependence of $\mathcal{E}_0(Pe)$ that motivates the development of a computational method that can handle singular source distributions.

In this study, for computational simplicity and efficiency, we utilize the 'random sine flow' as the stirring field. In the two-dimensional case this is defined for all time by

$$\boldsymbol{u}(t,\boldsymbol{x}) = \begin{cases} w\sin(2\pi y/L+\phi)\,\hat{\mathbf{i}}, & nT < t \le nT+\frac{1}{2}T; \\ w\sin(2\pi x/L+\phi')\,\hat{\mathbf{j}}, & nT+\frac{1}{2}T < t \le (n+1)T, \end{cases} \tag{13}$$

where T is the period, $n = 0,1,2,\ldots$, and ϕ and ϕ' are random phases chosen independently and uniformly on $[0,2\pi)$ in each half-cycle, which assures the homogeneity

J. Stat. Mech. (2008) P07018

of the flow field. In this case, $w = \sqrt{2}U$. In the three-dimensional case, we employ

$$\boldsymbol{u}(t,\boldsymbol{x}) = \begin{cases} w\left[\sin\alpha\sin\left(2\pi y/L+\phi_2\right)+\cos\alpha\sin\left(2\pi z/L+\phi_3\right)\right]\hat{\mathbf{i}}, \\ \qquad\qquad nT < t \le nT+\frac{1}{3}T; \\ w\left[\sin\alpha\sin\left(2\pi z/L+\psi_3\right)+\cos\alpha\sin\left(2\pi x/L+\phi_1\right)\right]\hat{\mathbf{j}}, \\ \qquad\qquad nT+\frac{1}{3}T < t \le nT+\frac{2}{3}T; \\ w\left[\sin\alpha\sin\left(2\pi x/L+\psi_1\right)+\cos\alpha\sin\left(2\pi y/L+\psi_2\right)\right]\hat{\mathbf{k}}, \\ \qquad\qquad nT+\frac{2}{3}T < t \le (n+1)T, \end{cases}$$

where again $w = \sqrt{2}U$, $n = 0, 1, 2, \ldots$, and α, $\phi_{1,2,3}$ and $\psi_{1,2,3}$ are uniform random numbers in $[0, 2\pi)$ chosen independently every $T/3$. The angle α randomizes the shear direction to guarantee statistical isotropy of the flow.

3. Numerical method

In a particle code for solving the advection–diffusion equation, the concentration field ρ is represented by a distribution of particles. Particles are introduced by generating random locations using the properly normalized source $S(\boldsymbol{x})$ as a probability distribution function, then they are transported by advection and diffusion. The particle density, $\rho(t,\boldsymbol{x})$, is measured by covering the domain with bins counting the number of particles per bin.

A discrete particle method is employed because it can easily deal with small scale sources such as δ functions. It is also straightforward to implement with any advection field. The downside of a particle method is that it necessarily involves two kinds of errors: the number density of particles calculated by dividing the domain into bins is only resolved down to the size of the bins, and the measurement of ρ always includes statistical errors due to the use of finite numbers of particles.

3.1. Time evolution

At each time step the system is evolved by advection, diffusion, the source, and sinks. An advection-only equation would be solved by moving particles along characteristics, and a diffusion-only equation would be solved by adding independent Gaussian noises to each coordinate of each particle. With both advection and diffusion we need to solve a stochastic differential equation to determine the proper displacement of the particles during a time step. The stochastic differential equation is

$$\mathrm{d}\boldsymbol{X} = \boldsymbol{u}(t,\boldsymbol{X})\,\mathrm{d}t + \sqrt{2\kappa}\,\mathrm{d}\boldsymbol{W}, \tag{14}$$

where $\boldsymbol{W}(t)$ is a standard vector-valued Wiener process.

In order to solve (14), we will consider cases where the displacement due to the noise in a subinterval of length T/d (where d is the dimension) is much smaller than the wavelength of the random sine flow. This condition is realized better and better as Pe increases. Then, during each subinterval, the drift field $\boldsymbol{u}(t,\boldsymbol{X})$ experienced by each particle can be approximated by a steady flow with a linear shear. In 2D, for the first half of the period for a particle starting at $(x_0, y_0) = (X(t=0), Y(t=0))$ we

J. Stat. Mech. (2008) P07018

approximate (14) by

$$\begin{aligned} \mathrm{d}X &= w\sin(2\pi y_0/L+\phi)\,\mathrm{d}t + w\cos(2\pi y_0/L+\phi)\frac{2\pi}{L}(Y-y_0)\,\mathrm{d}t + \sqrt{2\kappa}\,\mathrm{d}W_1, \\ \mathrm{d}Y &= \sqrt{2\kappa}\,\mathrm{d}W_2, \end{aligned} \tag{15}$$

and for the second half of the period, starting from $(x_0', y_0') = (X(t=T/2), Y(t=T/2))$,

$$\begin{aligned} \mathrm{d}X &= \sqrt{2\kappa}\,\mathrm{d}W_1, \\ \mathrm{d}Y &= w\sin\left(2\pi x_0'/L+\phi'\right)\,\mathrm{d}t + w\cos(2\pi x_0'/L+\phi')\frac{2\pi}{L}(X-x_0')\,\mathrm{d}t + \sqrt{2\kappa}\,\mathrm{d}W_2. \end{aligned} \tag{16}$$

Therefore, during the first half-period we evolve the position of a particle through a time interval Δt (where $\Delta t \le T/2$ need *not* be small) by the map

$$\begin{aligned} x_0 &\to x_0 + w\sin(2\pi y_0/L+\phi)\Delta t + R_1, \\ y_0 &\to y_0 + R_2, \end{aligned} \tag{17}$$

where R_1 and R_2 satisfy

$$\begin{aligned} \mathrm{d}R_1 &= S_2 R_2\,\mathrm{d}t + \sqrt{2\kappa}\,\mathrm{d}W_1 \qquad (S_2 := 2\pi w L^{-1}\cos(2\pi y_0/L+\phi)), \\ \mathrm{d}R_2 &= \sqrt{2\kappa}\,\mathrm{d}W_2. \end{aligned} \tag{18}$$

The variance–covariance matrix of R_1 and R_2 is

$$\begin{pmatrix} \boldsymbol{E}(R_1^2) & \boldsymbol{E}(R_1R_2) \\ \boldsymbol{E}(R_2R_1) & \boldsymbol{E}(R_2^2) \end{pmatrix} = \begin{pmatrix} \frac{2}{3}S_2^2\kappa t^3 + 2\kappa t & S_2\kappa t^2 \\ S_2\kappa t^2 & 2\kappa t \end{pmatrix}, \tag{19}$$

which is realized by

$$R_1 = \sqrt{\tfrac{1}{6}S_2^2\kappa t^3 + 2\kappa t}\times N_1 + \sqrt{\tfrac{1}{2}S_2^2\kappa t^3}\times N_2, \tag{20}$$

$$R_2 = \sqrt{2\kappa t}\times N_2, \tag{21}$$

where N_1 and N_2 are independent $N(0,1)$ random variables (normally distributed with mean 0 and standard deviation 1). The matrix (19) describes the evolution of a passive scalar field in a shear flow [28]–[30].

Therefore the time evolution map during the first half-period is

$$x_0 \to x_0 + w\sin\left(2\pi y_0/L+\phi\right)\,\Delta t + \sqrt{\tfrac{1}{6}S_2^2\kappa(\Delta t)^3 + 2\kappa\Delta t}\,N_1 + \sqrt{\tfrac{1}{2}S_2^2\kappa(\Delta t)^3}\,N_2, \tag{22a}$$

$$y_0 \to y_0 + \sqrt{2\kappa\Delta t}\,N_2. \tag{22b}$$

A similar map is employed during the second half of the period. These stochastic maps include the shear—in the approximation that the shear remains constant for each particle during each half-cycle—that causes a 'distortion' of a Gaussian cloud of particles; see figure 1.

J. Stat. Mech. (2008) P07018

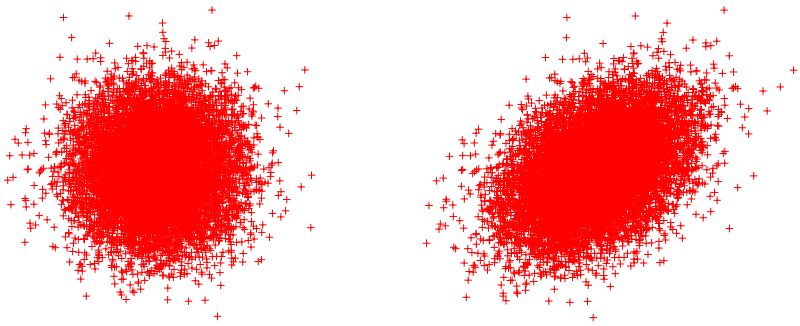

(a) (b)

Figure 1. (a) A circular Gaussian distribution of particles transported and sheared into (b) an elliptical Gaussian cloud.

The same calculations apply for the three-dimensional case: for the first subinterval, the time evolution map is

$$x_0 \to x_0 + w[\sin\alpha \sin(2\pi y_0/L + \phi_2) + \cos\alpha \sin(2\pi z_0/L + \phi_3)] + \sqrt{\tfrac{1}{6}({S_2}^2 + {S_3}^2)\kappa(\Delta t)^3 + 2\kappa\Delta t}\, N_1 + S_2\sqrt{\tfrac{1}{2}\kappa}(\Delta t)^{3/2}\, N_2 + S_3\sqrt{\tfrac{1}{2}\kappa}(\Delta t)^{3/2}\, N_3, \quad (23a)$$

$$y_0 \to y_0 + \sqrt{2\kappa\Delta t}\, N_2, \quad (23b)$$

$$z_0 \to z_0 + \sqrt{2\kappa\Delta t}\, N_3, \quad (23c)$$

where $S_2 = 2\pi w L^{-1} \sin\alpha \cos(2\pi y_0/L + \phi_2)$, $S_3 = 2\pi w L^{-1} \cos\alpha \cos(2\pi z_0/L + \phi_3)$, and N_1, N_2 and N_3 are independent $N(0,1)$ random variables. The maps for the other subintervals can be obtained by cyclic permutation of the coordinates.

The steady scalar source is realized by introducing new particles one by one using normalized $S(\boldsymbol{x})$ as a probability distribution function. Numerically, such a probability distribution function can be realized by mapping uniform random numbers over $[0,1]$ with the inverse of the cumulative probability distribution function in question.

New particles are added constantly so the total number of particles continues to increase, which slows down the computation. To cope with increasing numbers of particles, we implement a particle subtraction scheme. Particles eventually get well mixed and 'older' particles do not contribute to the value of the hydrodynamic variance. There is no added value in keeping track of particles that have been in the mix for a very long time, and we can simply remove them from the system after a sufficiently long time. It is very important to keep track of the 'age' of each particle, however, and to only remove sufficiently old well-mixed particles. (For example, if a random fraction of particles are removed at regular time intervals, then the simulation becomes one of a system of particles with a random finite lifetime, described by an advection–diffusion equation with an additional density decay term.)

In order to determine how old particles must be in order to safely remove them without affecting the hydrodynamic variance, prior to a full simulation run a test is performed as

J. Stat. Mech. (2008) P07018

follows. Starting from an initial set of N_i particles located in space according to the source distribution, the flow and diffusion are allowed to act and the variance of the number of particles per bin, which decays with time, is monitored. The number N_i is of the order of the number of particles that are introduced in the full simulation during, say, an interval of length T characteristic of the random sine flow. The variance does not decay all the way to zero, however, but rather to the variance expected when N_i particles are randomly distributed among the bins. The time when the variance achieves this random-distribution variance, measured beforehand for a given flow and diffusion strength, is then the required 'ageing' time before particles can be safely removed in the full simulation with the steady source. Such a trial run is performed for each flow, diffusion strength, source distribution and particle number because this 'mixing time' depends on all these factors. Further details of the criteria for removing old particles and extensive tests and benchmark trials may be found in [31].

3.2. Variance calculation and background noise

The variance $\langle\theta^2\rangle$ is measured by monitoring the fluctuations in the number of particles per bin, and time averaging. In d dimensions the domain is divided into l^d bins and the code calculates $\langle n^2\rangle$, where n is the number of particles in a bin. Then $\langle\theta^2\rangle$ is initially approximated by

$$\langle n^2\rangle - \langle n\rangle^2 = (L/l)^{2d}\,\langle\theta^2\rangle. \tag{24}$$

We say 'initially' because the expression above includes both the hydrodynamic fluctuations of interest *and* discreteness fluctuations resulting solely from the fact that each bin contains a finite number of particles.

The subtraction scheme eliminates the 'well-mixed' particles that do not contribute to the value of the hydrodynamic variance. But even if the system were completely mixed so that theoretically, $\langle\theta^2\rangle = 0$, the measured variance $\langle n^2\rangle - \langle n\rangle^2$ would be (very close to, for small bins) $\langle n\rangle$, which is on the order of N/l^d, where N is the total number of particles in the domain. This follows from the fact that $\theta(t, \boldsymbol{x})$ is represented in this particle method by only a finite number of particles in each finite-size bin. That is, $\langle\theta^2\rangle$ as defined by (24) is non-zero even when the particles are uniformly distributed: then the bulk variance includes fluctuations as if N particles were randomly thrown in l^d bins. The helpful fact is that the bulk variance contribution from these *background fluctuations* due to finite numbers of particles in the bins does not depend on (i.e., is uncorrelated with) the hydrodynamic density variation from bin to bin. The total contribution to the variance is the sum of the 'extra' variances in each of the bins which is linear in the (mean) number of particles in each bin. Hence the sum of the variances is $\sim N$ and the bulk variance contribution from the background fluctuations, Nl^d/L^{2d}, can simply be subtracted from the initial estimate for $\langle\theta^2\rangle$ in (24). The net result is our measured value of the hydrodynamic variance.

In addition to the inevitable fluctuations due to discreteness, density variations are observed only down to the length scales $\sim L/l$ because of the binning density, which is another source of error in this procedure. We use $l \geq 100$, which tests and benchmark studies indicate is sufficient for the examples studied here [31].

The variance is calculated once for each subinterval, and the instant when it is calculated is determined randomly in order to obtain an unbiased time average. Thus

J. Stat. Mech. (2008) P07018

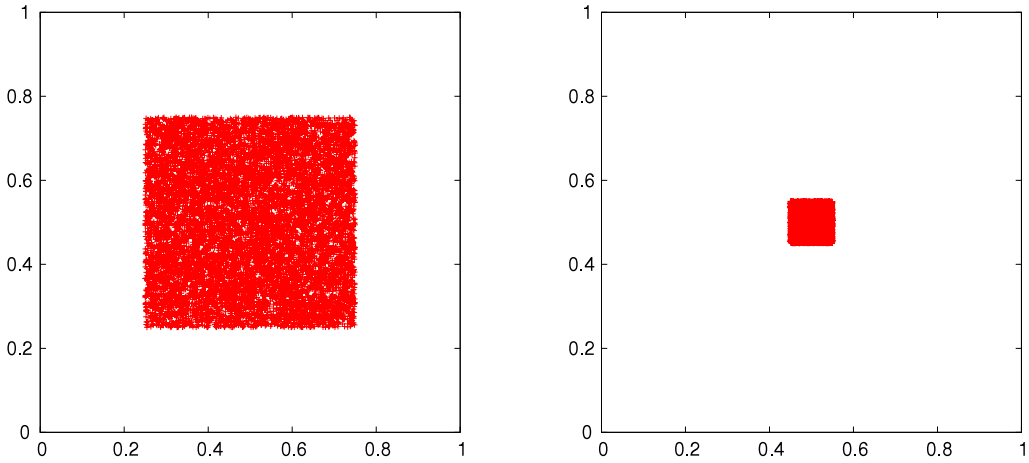

(a) $a = L/2$ (b) $a = L/10$

Figure 2. Square-shaped source of two different sizes; particles shown sampled from the uniform source distribution over the squares.

each subinterval is divided into two parts, before and after variance calculation, and the particle transport and source processes are appropriately adapted. The final measured quantities are long time averages that are observed to have converged to within the error indicated on the plots below.

4. Results

In order to investigate the effect of source–sink scales on maximal and actual mixing enhancements, we performed a series of calculations and simulations for square-shaped sources of various sizes $a < L$ as illustrated in figure 2.

Figure 3 shows the upper bounds on $\mathcal{E}_0$ for square sources and a δ-function source in 2D computed from (11). The upper bound for any finite-size source is asymptotically $\sim Pe$, but for the δ-function source it is $\sim Pe/\ln Pe$ in the large Pe limit. In 3D, the distinction between cubic sources and a δ-function source is more apparent as shown in figure 3(b): the upper bound for a δ-function source behaves $\sim\sqrt{Pe}$ in 3D. We stress that these mixing enhancement bounds apply for *any* statistically homogeneous and isotropic flows stirring sources with these shapes.

Simulation results for the random sine flow shown in figure 4(a) for 2D and figure 4(b) for 3D qualitatively confirm the behavior of the enhancements suggested by the upper limits. As the source size shrinks, the measured mixing enhancement gets smaller in a way that is remarkably similar to the bounds. In these simulations Pe is varied by decreasing κ at a fixed values of L, U and T. Other values of T and other (shorter) wavelengths of the stirring flow were also checked, producing similar plots. These 2D simulation results have recently been confirmed quantitatively by a PDE computation [32].

The simulations also show that the upper estimates can give the correct *quantitative* behavior of $\mathcal{E}_0$ as a function of Pe. Indeed, in figure 5 we plot the upper bound on $\mathcal{E}_0$ for the δ-function source in 3D and the measured enhancement from the simulations. The upper bound, which scales anomalously, $\sim\sqrt{Pe}$, is an excellent predictor of the data.

J. Stat. Mech. (2008) P07018

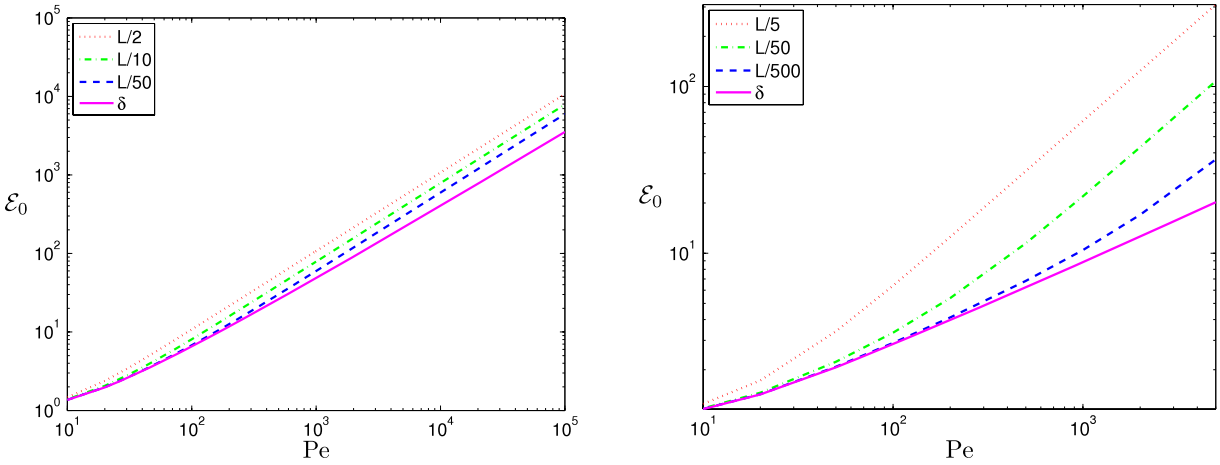

(a) $d = 2$ (b) $d = 3$

Figure 3. The theoretical upper bounds for (a) square sources with sizes $a = L/2, L/10, L/50$, and a δ-function source; (b) cubic sources with sizes $a = L/5, L/50, L/500$, and a δ-function source (from top to bottom).

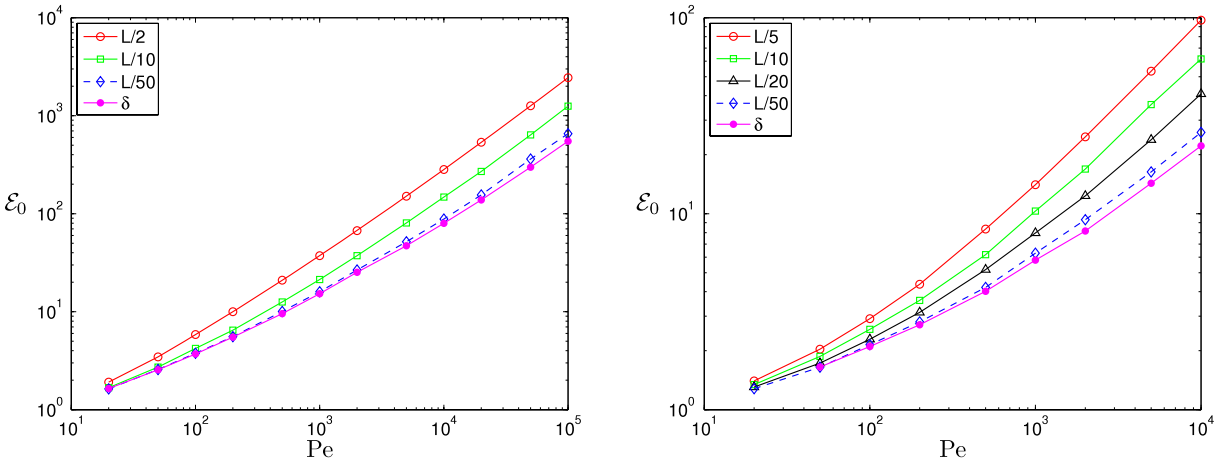

(a) $d = 2$ (b) $d = 3$

Figure 4. Measured mixing enhancements for (a) square sources with sizes $a = L/2, L/10, L/50$ and a δ-function source, (b) cubic sources with sizes $a = L/5, L/50, L/500$ and a δ-function source (from top to bottom).

From this we conclude that the random sine flow is an 'almost-optimal' mixer (among statistically homogeneous and isotropic flows) for this source–sink distribution.

5. Summary and conclusions

We have devised an accurate and computationally efficient particle method for studying hydrodynamic variance suppression by a mixing flow. Rigorous upper bounds for the

J. Stat. Mech. (2008) P07018

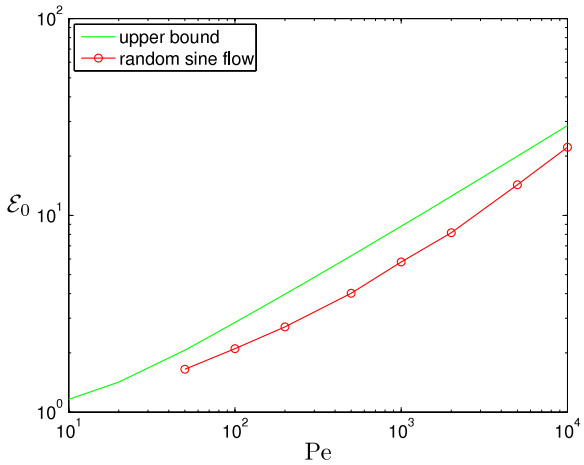

Figure 5. Mixing enhancement for a δ-function source in 3D. The solid line is the upper bound for any SHI flow and the data are mixing enhancements for the random sine flow measured in the discrete particle simulations.

mixing enhancement $\mathcal{E}_0$, i.e., the effective diffusion enhancement factor, were compared to measured enhancements for the simple random sine flow. A key prediction of the analysis in [24, 25] is that the source–sink shape is a determining factor in the mixing enhancement of any flow. The simulation results reported here show that the upper estimates give the correct qualitative picture as regards the Pe and source-shape dependence of $\mathcal{E}_0$.

Future work should focus on investigating enhancements of other stirring flows. No attempt has been made here to find a more efficient stirring flow (or, indeed, the *most* efficient flow, if there is one) whose enhancement approaches more closely (or perhaps even saturates) the upper bound. It is remarkable that the simple random sine flow appears to saturate the upper bound scaling $\mathcal{E}_0 \sim \sqrt{Pe}$ in 3D.

Stirring with appropriate turbulent solutions to the Navier–Stokes equation is also of significant interest. The central question here is, is statistically homogeneous and isotropic turbulence generically an efficient mixer? The answer may depend on the source–sink distribution.

Acknowledgments

The authors thank Jai Sukhatme for helpful comments on the paper. This work was supported in part by US National Science Foundation through awards PHY-0555324 and DMS-0553487, by US Department of Energy Contract DE-FG03-96ER-54346, by the Geophysical Fluid Dynamics Program at Woods Hole Oceanographic Institution, and by the Alexander von Humboldt Foundation.

References

[1] Ottino J M, *Mixing, chaotic advection, and turbulence*, 1990 *Annu. Rev. Fluid Mech.* **22** 207
[2] Majda A J and Kramer P R, *Simplified models for turbulent diffusion: theory, numerical modelling and physical phenomena*, 1999 *Phys. Rep.* **314** 237
[3] Warhaft Z, *Passive scalars in turbulent flows*, 2000 *Annu. Rev. Fluid Mech.* **32** 203
[4] Shraiman B I and Siggia E D, *Scalar turbulence*, 2000 *Nature* **405** 639
[5] Sawford B L, *Turbulent relative dispersion*, 2001 *Annu. Rev. Fluid Mech.* **33** 289

J. Stat. Mech. (2008) P07018

[6] Falkovich G, Gawędzki K and Vergassola M, *Particles and fields in turbulence*, 2001 *Rev. Mod. Phys.* **73** 913
[7] Aref H, *The development of chaotic advection*, 2002 *Phys. Fluids* **14** 1315
[8] Wiggins S and Ottino J M, *Foundations of chaotic mixing*, 2004 *Phil. Trans. R. Soc. Lond.* A **362** 937
[9] Thiffeault J-L, Doering C R and Gibbon J D, *A bound on mixing efficiency for the advection–diffusion equation*, 2004 *J. Fluid Mech.* **521** 105
[10] Townsend A A, *The diffusion of heat spots in isotropic turbulence*, 1951 *Proc. R. Soc. Lond.* A **209** 418
[11] Townsend A A, *The diffusion behind a line source in homogeneous turbulence*, 1954 *Proc. R. Soc. Lond.* A **224** 487
[12] Durbin P A, *A stochastic model of two-particle dispersion and concentration fluctuations in homogeneous turbulence*, 1980 *J. Fluid Mech.* **100** 279
[13] Drummond I T, *Path-integral methods for turbulent diffusion*, 1982 *J. Fluid Mech.* **123** 59
[14] Sawford B L and Hunt J C R, *Effects of turbulence structure, molecular diffusion and source size on scalar fluctuations in homogeneous turbulence*, 1986 *J. Fluid Mech.* **165** 373
[15] Thomson D J, *A stochastic model for the motion of particle pairs in isotropic high-Reynolds number turbulence, and its application to the problem of concentration variance*, 1990 *J. Fluid Mech.* **210** 113
[16] Borgas M S and Sawford B L, *A family of stochastic models for two-particle dispersion in isotropic homogeneous stationary turbulence*, 1994 *J. Fluid Mech.* **279** 69
[17] Chertkov M, Falkovich G, Kolokolov I and Lebedev V, *Statistics of a passive scalar advected by a large-scale two-dimensional velocity field: analytic solution*, 1995 *Phys. Rev.* E **51** 5609
[18] Chertkov M, Falkovich G, Kolokolov I and Lebedev V, *Normal and anomalous scaling of the fourth-order correlation function of a randomly advected passive scalar*, 1995 *Phys. Rev.* E **52** 4924
[19] Chertkov M, Kolokolov I and Vergassola M, *Inverse cascade and intermittency of passive scalar in one-dimensional smooth flow*, 1997 *Phys. Rev.* E **56** 5483
[20] Chertkov M, *Instanton for random advection*, 1997 *Phys. Rev.* E **55** 2722
[21] Chertkov M, Falkovich G and Kolokolov I, *Intermittent dissipation of a passive scalar in turbulence*, 1998 *Phys. Rev. Lett.* **80** 2121
[22] Balkovsky E and Fouxon A, *Universal long-time properties of Lagrangian statistics in the Batchelor regime and their application to the passive scalar problem*, 1999 *Phys. Rev.* E **60** 4164
[23] Plasting S and Young W R, *A bound on scalar variance for the advection–diffusion equation*, 2006 *J. Fluid Mech.* **552** 289
[24] Doering C R and Thiffeault J-L, *Multiscale mixing efficiencies for steady sources*, 2006 *Phys. Rev.* E **74** 025301(R)
[25] Shaw T A, Thiffeault J-L and Doering C R, *Stirring up trouble: Multi-scale mixing measures for steady scalar sources*, 2007 *Physica* D **231** 143
[26] Thiffeault J-L and Pavliotis G A, *Optimizing the source distribution in fluid mixing*, 2008 *Physica* D **237** 918
[27] Shaw T A, *Bounds on multiscale mixing efficiencies*, 2005 *Proc. 2005 Summer Program in Geophysical Fluid Dynamics* (Woods Hole, MA: Woods Hole Oceanographic Institute) p 291 http://www.whoi.edu/cms/files/Shaw_21281.pdf
[28] Taylor G I, *The dispersion of matter in turbulent flow through a pipe*, 1954 *Proc. R. Soc. Lond.* A **223** 446
[29] Aris R, *On the dispersion of a solute in a fluid flowing through a tube*, 1956 *Proc. R. Soc. Lond.* A **235** 67
[30] Rhines P B and Young W R, *How rapidly is a passive scalar mixed within closed streamlines?*, 1983 *J. Fluid Mech.* **133** 133
[31] Okabe T, *A particle-simulation method to study mixing efficiencies*, 2006 *Proc. 2006 Summer Program in Geophysical Fluid Dynamics* (Woods Hole, MA: Woods Hole Oceanographic Institute) http://www.whoi.edu/cms/files/Taka_21241.pdf
[32] Chertock A, Kashdan E, Kurganov A and Doering C R, *A fast explicit operator splitting method for passive scalar advection by a random stirring field*, 2008 *ESAIM: Mathematical Modelling and Numerical Analysis* submitted, available at http://math.tulane.edu/∼kurganov/Chertock-Doering-Kashdan-Kurganov.pdf

J. Stat. Mech. (2008) P07018